JOC Article

Intrinsic Conformational Characteristics of α,α-Diphenylglycine

Jordi Casanovas,*,† David Zanuy,‡ Ruth Nussinov,§,|| and Carlos Alemán*,‡

Departament de Química, Escola Politècnica Superior, Universitat de Lleida, c/Jaume II No. 69, Lleida E-25001, Spain, Departament d'Enginyeria Química, E. T. S. d'Enginyeria Industrial de Barcelona, Universitat Politècnica de Catalunya, Diagonal 647, Barcelona E-08028, Spain, Basic Research Program, SAIC-Frederick, Inc., Center for Cancer Research Nanobiology Program, NCI, Frederick, Maryland 21702, and Department of Human Genetics Sackler, Medical School, Tel Aviv University, Tel Aviv 69978, Israel

jcasanovas@quimica.udl.es; carlos.aleman@upc.edu

Received December 5, 2006

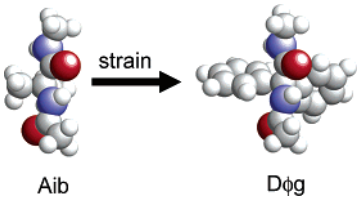

Quantum mechanical calculations at the B3LYP/6-31+G(d,p) level have been used to investigate the intrinsic conformational preferences of α,α-diphenylglycine, a simple α,α-dialkylated amino acid bearing two phenyl substituents on the α-carbon, in both the gas phase and aqueous solution. Nine minimum energy conformations have been characterized for the *N*-acetyl-*N*′-methylamide derivative within a relative energy range of about 9 kcal/mol. The relative stability of these structures is largely influenced by specific backbone···side chain and side chain···side chain interactions that can be attractive (N−H···π and C−H···π) or repulsive (C═O···π). On the other hand, comparison with the minimum energy conformations calculated for α-aminoisobutyric acid, in which the two phenyl substituents are replaced by methyl groups, revealed that the bulky aromatic rings of α,α-diphenylglycine induce strain in the internal geometry of the peptide. Finally, a set of force-field parameters for classical Molecular Mechanics calculations was developed for the investigated amino acid. Molecular Dynamics simulations in aqueous solutions have been carried out to validate the parameters obtained.

Introduction

The development of synthetic amino acids with restricted conformational properties represents an important goal of many researchers working in the field of peptide and protein rational design.[1−7] Now the interest in nonproteogenic amino acids with restricted backbone conformational mobility has been extended to the de novo approaches used in nanobiology. For instance, it was recently proposed to re-engineer protein modules via targeted replacements with conformationally constrained amino acids for the generation of nanodevices.[8] More specifically, to enhance the thermodynamic stability of the nanotubular structures constructed by self-assembling protein fragments with a β-helical conformation, the insertion of chemically constrained residues with suitable backbone conformational tendencies was recommended.[9]

† Universitat de Lleida.
‡ Universitat Politècnica de Catalunya.
§ Center for Cancer Research Nanobiology Program.
|| Tel Aviv University.

(1) Hruby, V. J.; Bonner, G. G. In *Methods in Molecular Biology*; Pennington, M. W., Dunn, B. M., Eds.; Humana Press, Inc.: Totowa, NJ, 1994; Vol. 35, pp 201−240.
(2) Rizo, J.; Gierasch, L. M. *An. Rev. Biochem.* **1992**, *61*, 387.
(3) Venkatraman, J.; Shankaramma, S. C.; Balaram, P. *Chem. Rev.* **2001**, *101*, 3131.
(4) Hill, D. J.; Mio, M. J.; Prince, R. B.; Hughes, T. S.; Moore, J. S. *Chem. Rev.* **2001**, *101*, 3893.
(5) Toniolo, C.; Crisma, M.; Formaggio, F.; Peggion, C. *Biopolymers (Pept. Sci.)* **2001**, *60*, 396.
(6) Cowell, S. M.; Lee, Y. S.; Cain, J. P.; Hruby, V. J. *Curr. Med. Chem.* **2004**, *11*, 2785.
(7) Wang, L.; Schultz, P. G. *Angew. Chem.* **2005**, *117*, 34; *Angew. Chem., Int. Ed.* **2005**, *44*, 34.
(8) Alemán, C.; Zanuy, D.; Jiménez, A. I.; Cativiela, C.; Haspel, N.; Zheng, J.; Casanovas, J.; Wolfson, H.; Nussinov, R. *Phys. Biol.* **2006**, *3*, S54.
(9) Haspel, N.; Zanuy, D.; Alemán, C.; Wolfson, H.; Nussinov, R. *Structure* **2006**, *14*, 1137.

10.1021/jo0624905 CCC: $37.00
Published on Web 02/10/2007

In recent studies, we investigated the intrinsic conformational properties of 1-aminocycloalkane-1-carboxylic acids (Ac_nc, where n indicates the size of the ring).[10−14] These synthetic amino acids are the result of $C^{\alpha}\leftrightarrow C^{\alpha}$ cyclization whereby dialkylated glycine residues with cyclic side chains are formed. Specifically, the structural and electronic characteristics of Ac_nc with $n = 3$,[10−12] 4,[13] and 5[14] were fully characterized using quantum mechanical methods. Results indicated that the backbone flexibility of Ac_nc is very low due not only to the $C^{\alpha,\alpha}$-disubstitution but also to the strain imposed by the cyclic side chain, even though such flexibility increases with the size of the ring.[10−14] On the other hand, the conformational preferences produced by the incorporation of one or more selectively oriented phenyl groups to the cyclopropane ring of Ac_3c were investigated using the same theoretical procedures,[12,15,16] with the results being fully consistent with experimental observations.[17−19] Interestingly, these compounds, which should be considered as cyclopropane phenylalanine (Phe) analogues, showed new stereochemical constraints that were produced by the interactions between the rigidly held aromatic side chains and the peptide backbone.

On the other hand, the intrinsic conformational preferences of α-aminoisobutyric acid (Aib), which is the simplest α,α-dialkylated amino acid, has been extensively investigated due to its strong helix-inducing properties.[10,20,21] Quantum mechanical calculations indicated that Aib, which is the linear homologue of Ac_3c, tends to adopt folded conformations.[10] Indeed, comparison of the results obtained at a similar computational level for Aib and alanine (Ala) dipeptides indicated that the incorporation of the second methyl group reduces the flexibility of the backbone, the conformational freedom of the former amino acid being more restricted than that of the latter.[10,22] Thus, the helix propensity of Aib was found to be several times larger than of Ala.

In this work, we investigate the conformational preferences of α,α-diphenylglycine residue (Dϕg) using quantum mechanical calculations. Thus, although this residue has been crystallized in both folded and extended conformations depending on the peptide sequence,[23−26] its intrinsic conformational tendencies have not been established yet. Accordingly, our aim is to ascertain the effects of the phenyl groups in the conformational preferences of linear α,α-dialkylated amino acids. The results provided in this paper are organized as follows. First, the potential energy surface of the *N*-acetyl-*N*′-methylamide derivative of Dϕg (Ac-Dϕg-NHMe) has been systematically explored using density functional theory (DFT) calculations. After this, the influence of the polarity of the environment on the conformational preferences of this dipeptide has been examined using a self-consistent reaction-field (SCRF) method. Next, the influence of the phenyl side groups in the conformational properties of Dϕg has been examined by comparing the minimum energy conformations of this amino acid with those of both Aib and cyclopropane Phe analogues. Finally, a set of force-field parameters has been developed for Dϕg to allow molecular dynamics simulations (MD). The conformational preferences predicted by MD simulations for Ac-Dϕg-NHMe have been compared with those obtained using DFT calculations to prove the suitability of such parameters.

Methods

All calculations were carried out using the Gaussian 03 computer program.[27] DFT calculations were performed using the following combination: the Becke's three-parameter hybrid functional (B3)[28] with the Lee, Yang, and Parr (LYP)[29] expression for the nonlocal correlation (B3LYP). Thus, all of the calculations presented in this work were performed using the B3LYP method combined with the 6-31+G(d,p) basis set.[30]

Torsion angles for the backbone and side chains of Ac-Dϕg-NHMe are defined in Figure 1. Because each flexible backbone dihedral angle is expected to have three minima, i.e., gauche$^+$ (60°), trans (180°), and gauche$^-$ (−60°), the number of minima that may be anticipated for the potential energy hypersurface $E = E(\varphi,\psi,\chi_1^0,\chi_1^1)$ of Ac-Dϕg-NHMe is $3^4 = 81$. However, due to the absence of stereochemistry, the number of theoretical minima can be reduced to 41, since $\{\varphi,\psi,\chi_1^0,\chi_1^1\} = \{-\varphi,-\psi,-\chi_1^0,-\chi_1^1\}$. Accordingly, the 41 structures were considered as starting points for complete geometry optimizations at the B3LYP/6-31+G(d,p) level. This systematic conformational analysis strategy has allowed us satisfactory exploration of the potential energy hypersurfaces not only of small dipeptides[10−16] but also of flexible organic molecules.[31,32]

(10) Alemán, C. *J. Phys. Chem. B.* **1997**, *101*, 5046.
(11) Gómez-Catalán, J.; Alemán, C.; Pérez, J. J. *Theor. Chem. Acc.* **2000**, *103*, 380.
(12) Alemán, C.; Jiménez, A. I.; Cativiela, C.; Pérez, J. J.; Casanovas, J. *J. Phys. Chem. B.* **2002**, *106*, 11849.
(13) Casanovas, J.; Zanuy, D.; Nussinov, R.; Alemán, C. *Chem. Phys. Lett.* **2006**, *429*, 558.
(14) Alemán, C.; Zanuy, D.; Casanovas, J.; Cativiela, C.; Nussinov, J. *J. Phys. Chem. B* **2006**, *110*, 21264.
(15) Casanovas, J.; Jiménez, A. I.; Cativiela, C.; Pérez, J. J.; Alemán, C. *J. Org. Chem.* **2003**, *68*, 7088.
(16) Casanovas, J.; Jiménez, A. I.; Cativiela, C.; Pérez, J. J.; Alemán, C. *J. Phys. Chem. B* **2006**, *110*, 5762.
(17) Jiménez, A. I.; Cativiela, C.; Aubry, A.; Marraud, M. *J. Am. Chem. Soc.* **1998**, *120*, 9452.
(18) Jiménez, A. I.; Vanderesse, R.; Marraud, M.; Aubry, A.; Cativiela, C. *Tetrahedron Lett.* **1997**, *38*, 7559.
(19) Jiménez, A. I.; Ballano, G.; Cativiela, C. *Angew. Chem., Int. Ed.* **2005**, *127*, 2036.
(20) Zhang, L.; Herman, J. *J. Am. Chem. Soc.* **1994**, *116*, 11915.
(21) Improta, R.; Rega, N.; Alemán, C.; Barone, V. *Macromolecules* **2001**, *34*, 7550.
(22) Gould, I. R.; Kollman, P. A. *J. Phys. Chem.* **1992**, *96*, 9255.
(23) Pavone, V.; Lombardi, A.; Saviano, M.; Di Blasio, B.; Nastri, F.; Fattorusso, R.; Zaccaron, L.; Maglio, O.; Yamada, T.; Omote, Y.; Kuwatam, S. *Biopolymers* **1994**, *34*, 1595.
(24) Crisma, M.; Valle, G.; Bonora, G. M.; Toniolo, C.; Lelj, F.; Barone, V.; Fraternali, F.; Hardy, P. M.; Maia, H. L. S. *Biopolymers* **1991**, *31*, 637.
(25) Toniolo, C.; Crisma, M.; Fabiano, N.; Melchiorri, P.; Negri, L.; Krause, J. A.; Eggleston, D. S. *Int. J. Pept. Prot. Res.* **1994**, *44*, 85.
(26) Pavone, V.; Lombardi, A.; Saviano, M.; Nastri, E.; Zaccaro, L.; Magio, O.; Pedone, C.; Omote, Y.; Yamanaka, Y.; Yamada, T. *J. Pept. Sci.* **1998**, *4*, 21.
(27) Gaussian 03, Revision B.02: Frisch, M. J.; Trucks, G. W.; Schlegel, H. B.; Scuseria, G. E.; Robb, M. A.; Cheeseman, J. R.; Montgomery, J. A.; Vreven, Jr., T.; Kudin, K. N.; Burant, J. C.; Millam, J. M.; Iyengar, S. S.; Tomasi, J.; Barone, V.; Mennucci, B.; Cossi, M.; Scalmani, G.; Rega, N.; Petersson, G. A.; Nakatsuji, H.; Hada, M.; Ehara, M.; Toyota, K.; Fukuda, R.; Hasegawa, J.; Ishida, M.; Nakajima, T.; Honda, Y.; Kitao, O.; Nakai, H.; Klene, M.; Li, X.; Knox, J. E.; Hratchian, H. P.; Cross, J. B.; Adamo, C.; Jaramillo, J.; Gomperts, R.; Stratmann, R. E.; Yazyev, O.; Austin, A. J.; Cammi, R.; Pomelli, C.; Ochterski, J. W.; Ayala, P. Y.; Morokuma, K.; Voth, G. A.; Salvador, P.; Dannenberg, J. J.; Zakrzewski, V. G.; Dapprich, S.; Daniels, A. D.; C. Strain, M.; Farkas, O.; Malick, D. K.; Rabuck, A. D.; Raghavachari, K.; Foresman, J. B.; Ortiz, J. V.; Cui, Q.; Baboul, A. G.; Clifford, S.; Cioslowski, J.; Stefanov, B. B.; Liu, G.; Liashenko, A.; Piskorz, P.; Komaromi, I.; Martin, R. L.; Fox, D. J.; Keith, T.; Al-Laham, M. A.; Peng, C. Y.; Nanayakkara, A.; Challacombe, M.; Gill, P. M. W.; Johnson, B.; Chen, W.; Wong, M. W.; Gonzalez, C.; Pople, J. A. Gaussian, Inc., Pittsburgh PA, 2003.
(28) Becke, A. D. *J. Chem. Phys.* **1993**, *98*, 1372.
(29) Lee, C.; Yang, W.; Parr, R. G. *Phys. Rev. B.* **1993**, *37*, 785.
(30) McLean, A. D.; Chandler, G. S. *J. Chem. Phys.* **1980**, *72*, 5639.
(31) Alemán, C.; Casanovas, J.; Zanuy, D.; Hall, H. K., Jr. *J. Org. Chem.* **2005**, *70*, 2950.
(32) Alemán, C.; Casanovas, J.; Hall, H. K., Jr. *J. Org. Chem.* **2005**, *70*, 7731.

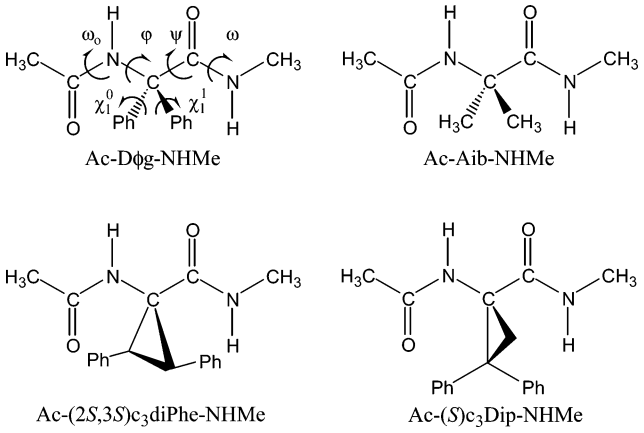

FIGURE 1. Chemical structure of the peptides examined in the present work. The minimum energy conformations of Ac-Dϕg-NHMe and Ac-Aib-NHMe have been characterized in this study at the B3LYP/6-31+G(d,p) level, while the potential energy hypersurfaces of Ac-(2*S*,3*S*)$c_3$diPhe-NHMe and Ac-(*S*)c_3Dip-NHMe were reported in refs 15 and 16, respectively.

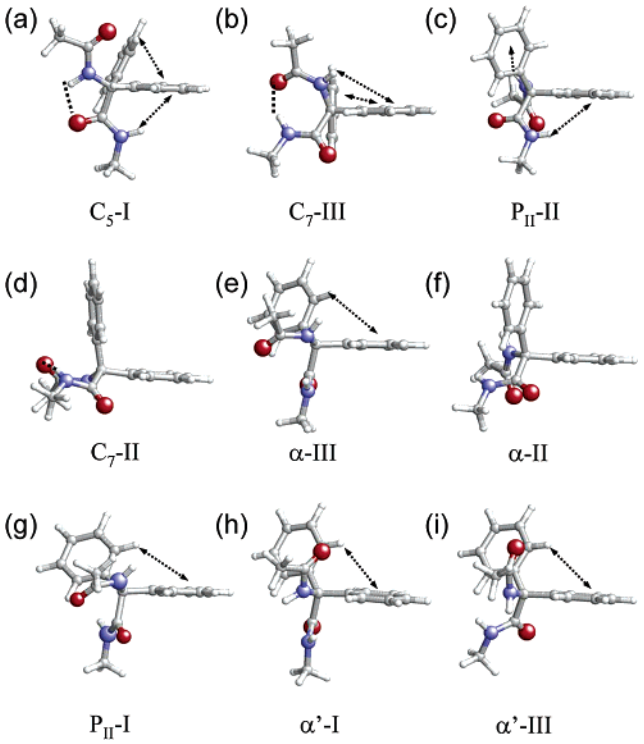

FIGURE 2. Minimum energy conformations of Ac-Dϕg-NHMe at the B3LYP/6-31+G(d,p) level. The labels used to identify the different minima are described in the text. Intramolecular hydrogen bonds (dashed lines) and both N−H···π and C−H···π interactions (dashed arrows) are indicated. The geometric parameters associated with the intramolecular interactions are given in the text.

Frequency analyses were carried out to verify the nature of the minimum state of all the stationary points obtained and to calculate the zero-point vibrational energies (ZPVE) and both thermal and entropic corrections. These statistical terms were used to compute the conformational Gibbs free energies in the gas phase (ΔG^{gp}) at the B3LYP/6-31+G(d,p) level.

In order to ascertain how the aromatic phenyl groups affect both the accessible backbone conformations of Ac-Dϕg-NHMe and the relative energy order of its minimum energy structures, the potential energy surface of the *N*-acetyl-*N*′-methylamide derivative of Aib (Ac-Aib-NHMe) was computed at the B3LYP/6-31+G(d,p) level. In Aib, which is the simplest α,α-dialkylated amino acid, small methyl groups replace the bulky phenyl rings (Figure 1). The theoretical methods used to investigate the conformational preferences of Ac-Aib-NHMe were identical to those described above for Ac-Dϕg-NHMe. However, in this case, only five conformations were used as starting points for geometry optimizations since the number of minima that may be anticipated for the potential energy hypersurface $E = E(\varphi,\psi)$ of Ac-Aib-NHMe is $3^2 = 9$ with four of them being 2-fold degenerated due to the achiral nature of Aib.

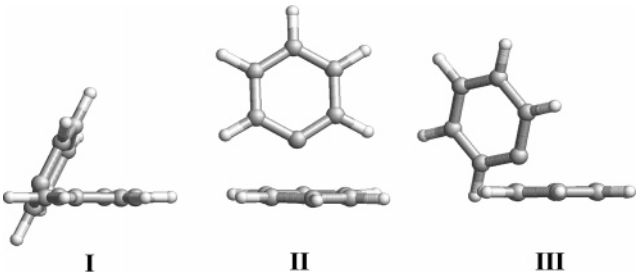

FIGURE 3. Relative arrangements of phenyl substituents found in the minimum energy conformations of Ac-Dϕg-NHMe.

To obtain estimation of the solvation effects on the relative stability of the different minima characterized for Ac-Dϕg-NHMe and Ac-Aib-NHMe, single-point calculations were also conducted on the B3LYP/6-31+G(d,p) optimized structures using a self-consistent reaction field (SCRF) model. The SCRF methods treat the solute at the quantum mechanical level, while the solvent is represented as a dielectric continuum. Specifically, we chose the polarizable continuum model (PCM) developed by Tomasi and co-workers to describe the bulk solvent.[33−35] The PCM method involves the generation of a solvent cavity from spheres centered at each atom in the molecule and the calculation of virtual point charges on the cavity surface representing the polarization of the solvent. The magnitude of these charges is proportional to the derivative of the solute electrostatic potential at each point calculated from the molecular wavefunction. The point charges may, then, be included in the one-electron Hamiltonian, thus inducing polarization of the solute. An iterative calculation is carried out until the wavefunction and the surface charges are self-consistent. PCM calculations were also performed in the framework of the DFT B3LYP/6-31+G(d,p) level using the standard protocol and considering the dielectric constant of water ($\epsilon = 78.4$). The conformational free energies in aqueous solutions (ΔG^{WAT}) were computed using the classical thermodynamics scheme: the free energy of solvation ($\Delta G_{sol/WAT}$) provided by the PCM model was added to the ΔG^{gp}.

$$\Delta G^{WAT} = \Delta G_{sol/WAT} + \Delta G^{gp} \quad (1)$$

MD simulations in water solutions were performed using the NAMD program.[36] The model peptide Ac-Dϕg-NHMe was placed in the center of a cubic simulation box ($a = 22.0$ Å) filled with 336 explicit water molecules, which were represented using the TIP3P model.[37] Atom pair distance cutoffs were applied at 12 Å to compute van der Waals interactions. The electrostatic interactions were computed using the nontruncated electrostatic potential by means of Ewald summations. The real space term was determined by the van der Waals cutoff (12 Å), while the reciprocal term was

(33) Miertus, M.; Scrocco, E.; Tomasi, J. *Chem. Phys.* **1981**, *55*, 117.
(34) Miertus, S.; Tomasi, J. *Chem. Phys.* **1982**, *65*, 239.
(35) Tomasi, J.; Mennucci, B.; Cammi, R. *Chem. Rev.* **2005**, *105*, 2999.
(36) Kale, L.; Skeel, R.; Bhandarkar, M.; Brunner, R.; Gursoy, A.; Krawetz, N.; Phillips, J.; Shinozaki, A.; Varadarajan, K.; Schulten, K. *J. Comp. Phys.* **1999**, *151*, 283.
(37) Jorgensen, W. L.; Chandrasekhar, J.; Madura, J. D.; Impey, R. W.; Klein, M. L. *J. Chem. Phys.* **1982**, *79*, 926.

TABLE 1. Backbone and Side Chain Torsion Angles[a] and Relative Energy[b] for the Minimum Energy Conformations of Ac−Dϕg-NHMe at the B3LYP/6-31+G(d,p) Level of Theory

conformer	ω_0	φ	ψ	ω	χ_1^0	χ_1^1	ΔE
C_5-I	174.0	172.2	−162.2	−179.0	77.5/−98.5	34.5/−151.5	0.0
C_7-III	−174.1	−68.7	48.5	175.3	26.4/−157.4	−115.4/62.4	1.1
P_{II}-II	163.2	−42.0	132.6	−173.9	165.3/−14.3	−65.3/114.2	2.4
C_7-II	−175.0	70.9	−75.8	172.5	31.8/−153.9	−30.9/155.4	3.7
α-III	−160.2	−64.4	−27.3	179.4	74.6/−99.7	21.1/−163.1	4.0
α-II	−173.9	−55.7	−32.8	175.5	176.2/−0.4	116.7/−63.4	5.7
P_{II}-I	175.8	−52.2	151.2	−179.7	−84.5/87.9	26.2/−160.1	6.2
α′-I	161.2	178.9	−31.5	−169.0	−80.6/93.1	−172.8/13.0	6.5
α′-III	174.4	160.5	−15.7	−174.4	3.4/176.0	111.3/68.1	9.8

[a] In degrees. See Figure 1. [b] In kcal/mol.

estimated by interpolation of the effective charge into a charges mesh with a grid thickness of 5 points per volume unit, i.e., the particle-mesh Ewald (PME) method.[38] All bond lengths were constrained along the MD using the *SHAKE* algorithm,[39] and the numerical integration step was 2 fs.

Before starting the MD run series, 5000 steps of energy minimization were performed to relax conformational and structural tensions. Different consecutive rounds of short MD runs were performed in order to equilibrate the density, temperature, and pressure: 0.4 ns of *NVT*-MD at 298 K (thermal relaxation) followed by 0.4 ns of isobaric relaxation (*NPT*-MD). Both temperature and pressure were controlled by the weak coupling method, the Berendsen thermobarostat[40] using a time constant for heat bath coupling, and a pressure relaxation time of 1 ps. The coordinates of the *NPT*-MD production runs, which were 25 ns long, were saved every 500 steps (1 ps intervals) for subsequent analysis.

Results and Discussion

Conformational Properties. Geometry optimizations in the gas phase at the B3LYP/6-31+G(d,p) level of the 41 structures considered as starting geometries led to nine different minimum energy structures for Ac-Dϕg-NHMe, which are 2-fold degenerated, i.e., the structures with $\{\varphi,\psi,\chi_1^0,\chi_1^1\}$ and $\{-\varphi,-\psi,-\chi_1^0,-\chi_1^1\}$ are equivalent and isoenergetic. Table 1 lists the backbone and side chain torsion angles of such minima, which are represented in Figure 2.

As is common in the conformational studies of nonchiral dipeptides, the backbone conformations were classified as follows: C_5 (five-membered intramolecular hydrogen-bonded ring; $\varphi,\psi \approx 180°,180°$), C_7 (seven-membered intramolecular hydrogen-bonded ring; $\varphi,\psi \approx 60°,-60°$ and $\varphi,\psi \approx -60°,60°$), P_{II} ($\varphi,\psi \approx -60°,180°$ and $\varphi,\psi \approx 60°,180°$), α ($\varphi,\psi \approx 60°,60°$ and $\varphi,\psi \approx -60°,-60°$), and α′ ($\varphi,\psi \approx 180°,60°$ and $\varphi,\psi \approx 180°,-60°$).[10−16,22,41] On the other hand, three relative arrangements were detected for side phenyl groups in Ac-Dϕg-NHMe minima, which were labeled as I, II, and III (Figure 3). In arrangement I, the rings are tilted, an intramolecular interaction being clearly detected between the C−H bond of the one phenyl and the π-cloud of the other, i.e., C−H···π interaction. No interaction appears in arrangement II, in which the two rings are relatively far forming an angle of ∼90°. Finally, although in arrangement III the angle between the two rings is also of ∼90°, a C−H···π interaction is clearly identified since one phenyl is rotated with respect to the other providing a suitable orientation for the formation of such intramolecular interaction, and in addition, the distance between them is small enough.

The lowest energy conformation in the gas-phase corresponds to the C_5−I (Figure 2a), in which the backbone dihedral angles φ,ψ define an intramolecular hydrogen bond with parameters d(H···O) = 2.024 Å and ∠N−H···O = 113.1° and the phenyl groups form the C−H···π interaction typically found in arrangements of type I. Additionally, an N−H···π interaction involving the N−H of the N-methylamide blocking group and one side phenyl group is detected in this conformation. The geometric parameters used to characterize the C−H···π and N−H···π interactions are as follows: (i) the distance between the hydrogen atom of the X−H moiety with X═C or N and the center of the ring ($d_{H\cdots Ph}$) and (ii) the angle defined by the X−H bond and the plane of the ring (θ). These parameters are [$d_{H\cdots Ph}$ = 3.462 Å, θ = 28.6°] and [$d_{H\cdots Ph}$ = 3.265 Å, θ = 31.7°] for the C−H···π and N−H···π interactions, respectively, the two sets of parameters being consistent with a partially tilted arrangement between the X−H bond and the phenyl ring.

In the next minimum, named as C_7-III (Figure 2b), the amide moieties define an intramolecular hydrogen bond with d(H···O) = 1.825 Å and ∠N−H···O = 153.2°, while the phenyl groups adopt an arrangement of type III forming a C−H···π interaction with parameters $d_{H\cdots Ph}$ = 3.462 Å and θ = 3.9°. Additionally, the second N−H moiety forms an N−H···π interaction with parameters $d_{H\cdots Ph}$ = 3.431 Å and θ = 10.4°. The third minimum corresponds to a P_{II}-II conformation (Figure 2c). This structure presents two N−H···π interactions with parameters [$d_{H\cdots Ph}$ = 3.174 Å, θ = 8.9°] and [$d_{H\cdots Ph}$ = 3.501 Å, θ = 11.1°], with no intramolecular hydrogen bond or C−H···π interaction being detected. The C_7-III and P_{II}-II minima are unfavored by 1.1 and 2.4 kcal/mol, respectively, with respect to the global minimum. The next minimum is the C_7-II (Figure 2d), which is destabilized by 3.7 kcal/mol with respect to the C_5-I. The only intramolecular interaction in this conformation is the hydrogen bond with parameters d(H···O) = 1.998 Å and ∠N−H···O = 138.7°, no X−H···π interaction with X = C or N being detected. This feature explains the unfavorable relative energy of C_7-II, which is 2.6 kcal/mol higher than that of C_7-III.

The relative energies of the remaining five minima range from 4.0 to 9.8 kcal/mol. This set of high energy structures contains (i) the α-III (Figure 2e) and α-II (Figure 2f) helical conforma-

(38) Darden, T.; York, D.; Pedersen, L. *J. Chem. Phys.* **1993**, *98*, 10089.
(39) Berendsen, H. J. C.; Postma, J. P. M.; van Gunsteren, W. F.; DiNola, A.; Haak, J. R. *J. Chem. Phys.* **1984**, *81*, 3684.
(40) Ryckaert, J. P.; Ciccotti, G.; Berendsen, H. J. C. *Comput. Phys.* **1990**, *94*, 1683.
(41) (a) Beachy, M. D.; Chasman, D.; Murphy, R. B.; Halgren, T. A.; Friesner, R. A. *J. Am. Chem. Soc.* **1997**, *119*, 5908. (b) Cornell, W. D.; Gould, I. R.; Kollman, P. A. *THEOCHEM* **1997**, *392*, 101. (c) Head-Gordon, T.; Head-Gordon, M.; Frisch, M. J.; Brooks, C. L., III; Pople, J. A. *J. Am. Chem. Soc.* **1991**, *113*, 5859. (d) Shang, H. S.; Head-Gordon, T. *J. Am. Chem. Soc.* **1994**, *116*, 1528. (e) Sulzbach, H. M.; Vacek, G.; Schreiner, P. R.; Morrison-Galbraith, J.; Schleyer, P. v. R.; Schaffer, H. F. J. *J. Comput. Chem.* **1997**, *18*, 126. (f) Alemán, C.; Puiggalí, J. *J. Phys. Chem. B.* **1997**, *101*, 3441.

TABLE 2. Relative Conformational Free Energies[a] at 298 K for the Minimum Energy Conformations of Ac-Dϕg-NHMe in the Gas-Phase and Aqueous Solution (ΔG^{gp} and ΔG^{WAT}, Respectively) (The Relative Solvation Free Energies[a] in Aqueous Solutions ($\Delta\Delta G_{sol/WAT}$) Are Also Displayed)

conformer	ΔG^{gp}	$\Delta\Delta G_{sol/WAT}$	ΔG^{WAT}
C_5-I	0.0	0.0	0.0
C_7-III	1.5	−0.5	1.0
P_{II}-II	2.8	−0.8	2.0
C_7-II	4.0	−0.6	3.4
α-III	4.1	0.1	4.2
α-II	4.8	−1.2	3.6
P_{II}-I	6.1	−1.8	4.3
α′-I	7.0	−0.4	6.6
α′-III	9.4	−1.5	7.9

[a] In kcal/mol.

tions, which differ in the arrangement of the phenyl groups (i.e., α-III presents a C−H···π interaction while none intramolecular interactions were found for α-II); (ii) the P_{II}-I conformation (Figure 2g), in which the two N−H···π interactions described above for P_{II}-II are replaced by a single C−H···π interaction; and (iii) the α′-I (Figure 2h) and α′-III (Figure 2i) conformations, which are stabilized by a single C−H···π interaction (i.e., no N−H···π interaction was detected). On the other hand, it is worth noting that the relative energy difference of the α′-III minimum is 3.3 kcal/mol higher than that of the previous minimum, which is the α′-I one. Inspection of Figure 2i indicates that such large destabilization arises from the unfavorable interaction between the lone pairs of the backbone C═O groups and the π-clouds of the side phenyl groups. Thus, the change in the arrangement of the phenyl groups from I to III induces small variations in the backbone dihedral angles of the α′ conformation originating such repulsive interactions.

Table 2 shows the conformational free energies at $T = 298$ K in the gas phase. As can be seen, the stability order provided by the relative energies listed in Table 1 was not altered by the addition of the ZPE, thermal, and entropic corrections. Thus, the value of such thermodynamical corrections was relatively small. The largest difference between ΔG^{gp} and ΔE^{gp}, which was detected for the α-II minimum, was 0.9 kcal/mol, such difference being smaller than 0.5 kcal/mol for the other eight minimum energy conformations. On the other hand, Table 2 also includes both the relative solvation energy and the relative conformational free energy at $T = 298$ K in aqueous solution, which was estimated according to eq 1. In general, the solvent plays a stabilizing role, which is reflected by the increase of the relative stabilities. The larger changes correspond to α-II, P_{II}-I and α′-III, which become 1.2, 1.8, and 1.5 kcal/mol, respectively, more stable in solution than in the gas phase. Regarding the order of the stabilities, the α-II is the only affected conformation becoming more stable than the α-III.

It is worth noting that the C_5-I and C_7-III are the only significant minima in both the gas phase and aqueous solution. The expected population of the remaining seven minima is negligible in these two environments since $\Delta G^{gp} > 2.8$ kcal/mol and $\Delta G^{WAT} > 2.0$ kcal/mol. Indeed, inclusion of solvent effects considerably enhances the population of C_7-III. Thus, according to the Boltzmann distribution used to describe the conformational preferences of small peptides, the population of C_7-III increases from 7.2% in the gas phase to 15.5% in aqueous solution.

Influence of the Phenyl Side Chains in the Conformational Properties. Calculations at the B3LYP/6-31+G(d,p) level on Ac-Aib-NHMe led to five minimum energy conformations, four of them being 2-fold degenerate. Table 3 lists the dihedral angles and relative energies of such minima, while the conformational free energies in both the gas phase and aqueous solution are displayed in Table 4.

TABLE 3. Torsion Angles[a] and Relative Energy[b] for the Minimum Energy Conformations of Ac-Aib-NHMe at the B3LYP/6-31+G(d,p) Level of Theory

conformer	ω_0	φ	ψ	ω	ΔE
C_7	−174.1	−72.9	55.4	179.1	0.0
C_5	180.0	180.0	180.0	180.0	0.4
P_{II}	170.4	−57.6	126.2	−175.3	2.6
α	−167.2	−69.3	−21.6	177.5	2.6
α′	169.7	173.1	−34.4	−172.3	4.5

[a] In degrees. See Figure 1. [b] In kcal/mol.

TABLE 4. Relative Conformational Free Energies[a] at 298 K for the Minimum Energy Conformations of Ac-Aib-NHMe in the Gas Phase and Aqueous Solution (ΔG^{gp} and ΔG^{WAT}, Respectively) (The Relative Solvation Free Energies[a] in Aqueous Solutions ($\Delta\Delta G_{sol/WAT}$) Are Also Displayed)

conformer	ΔG^{gp}	$\Delta\Delta G_{sol/WAT}$	ΔG^{WAT}
C_7	0.7	0.3	1.0
C_5	0.0	0.0	0.0
P_{II}	3.0	0.1	3.1
α	2.9	0.6	3.6
α′	4.6	0.6	5.2

[a] In kcal/mol.

TABLE 5. Energy Contribution Associated with the Phenyl Substituents[a] ($E^{Ph/Ph}$) for the Minimum Energy Conformations of Ac-Dϕg-NHMe in the Gas-Phase and Aqueous Solution

conformer	$E^{Ph/Ph}$ (gas phase)	$E^{Ph/Ph}$ (aqueous solution)
C_5-I	+13.4	+18.8
C_7-III	+14.3	+19.4
P_{II}-II	+13.3	+17.9
C_7-II	+16.8	+21.8
α-III	+14.6	+20.8
α-II	+15.3	+20.2
P_{II}-I	+16.6	+20.2
α′-I	+15.9	+21.4
α′-III	+18.3	+22.7

[a] In kcal/mol. $E^{Ph/Ph}$ was computed using eq 2 (see text).

The results obtained in this work for Ac-Aib-NHMe are in good agreement with those reported in an earlier study at the MP2/6-31G(d)//HF/6-31G(d) level of theory.[10] Thus, the C_7 is the lowest energy conformation, the C_5 being destabilized by 0.4 kcal/mol. However, this relative energy order is exchanged when the ZPE, thermal, and entropic corrections are added, as well as when solvent effects are included. Thus, the ΔG^{gp} and ΔG^{WAT} values of the C_7 are 0.7 and 1.0 kcal/mol, respectively, higher than those of the C_5. The hydrogen-bonding parameters calculated for the intramolecular hydrogen bonds of the C_5 and C_7 conformations are [d(H···O) = 2.032 Å, ∠N−H···O = 112.5°] and [d(H···O) = 1.897 Å, ∠N−H···O = 151.7°], respectively. On the other hand, the relative energy of the other three minimum energy conformations, which are unfavored by more than 2.5 kcal/mol, is α ≈ P_{II} < α′ and P_{II} < α < α′ in the gas phase and aqueous solution, respectively. Indeed, inspection of Table 4 reveals that the solvent increases the range of relative energies destabilizing the four local minima with respect to the C_5.

TABLE 6. $\angle N-C^{\alpha}-C$ and $\angle C^{\beta}-C^{\alpha}-C^{\beta'}$ Bond Angles[a] for the Minimum Energy Conformations of Ac-Dϕg-NHMe and Ac-Aib-NHMe

	Ac-Dϕg-NHMe			Ac-Aib-NHMe	
conformer	$\angle N-C^{\alpha}-C$	$\angle C^{\beta}-C^{\alpha}-C^{\beta'}$	conformer	$\angle N-C^{\alpha}-C$	$\angle C^{\beta}-C^{\alpha}-C^{\beta'}$
C_5-I	102.9	114.2	C_7	111.7	109.7
C_7-III	112.1	111.9	C_5	104.4	111.1
P_{II}-II	106.2	108.7	P_{II}	107.6	109.6
C_7-II	105.4	106.3	α	112.5	110.1
α-III	111.5	112.0	α'	107.9	110.7
α-II	109.7	108.4			
P_{II}-I	107.7	113.5			
α'-I	107.2	114.2			
α'-III	106.6	112.7			

[a] In degrees.

Figure 4 represents the position of all the minima characterized for Ac-Dϕg-NHMe and Ac-Aib-NHMe in the φ,ψ-Ramachandran map. As can be seen, with the exception of the C_5 (φ,ψ = 180°,180°), every minimum of Ac-Aib-NHMe spreads out in two minima when the methyl groups are replaced by phenyl rings. Such two minima present similar backbone conformations but different arrangements of the aromatic side chains. This result suggests that the substitution of the side groups does not produce significant changes in the backbone conformation. However, inspection to the relative energies of the different minima (Tables 2 and 4) reveals that the bulky phenyl groups introduce, in some cases, strong destabilizing effects due to unfavorable interactions. In order to evaluate these interactions from a quantitative point of view, the isodesmic reaction displayed in the following scheme has been considered.[42]

SCHEME 1

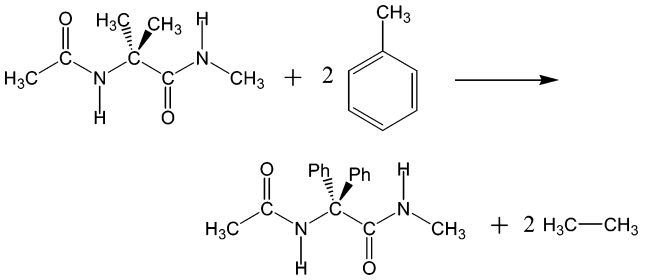

For each conformation of Ac−Dϕg-NHMe, the energy contribution associated with the phenyl substituents, $E^{Ph/Ph}$, was estimated according to eq 2

$$E^{Ph/Ph} = E^{Ac-D\phi g-NHMe} - [(E^{Ac-Aib-NHMe} - 2E^{H_3C-CH_3}) + 2E^{Ph-CH_3}] \quad (2)$$

where $E^{Ac-D\phi g-NHMe}$ is the electronic energy of the conformation under study and $E^{Ac-Aib-NHMe}$ is the electronic energy of the Ac-Aib-NHMe minimum with similar backbone conformation. The results are displayed in Table 5.

As can be seen, the values of $E^{Ph/Ph}$ reveal significant unfavorable effects for all of the minimum energy conformations of Ac-Dϕg-NHMe in both the gas phase and aqueous solution. These should be mainly attributed to both the strain energy induced by the phenyl side groups and the unfavorable interactions between the aromatic rings and the backbone C=O moieties. More specifically, the phenyl ring is a bulky group able to induce strain in the internal geometry of the peptide. This strain is clearly evidenced in Table 6, which compares the $\angle N-C^{\alpha}-C$ and $\angle C^{\beta}-C^{\alpha}-C^{\beta'}$ bond angles of the minimum energy conformations of Ac-Dϕg-NHMe and Ac-Aib-NHMe. As can be seen, the deviation with respect to the value ideally expected for these angles (109.5°) is higher for Ac-Dϕg-NHMe than for Ac-Aib-NHMe. On the other hand, the phenyl groups present a large amount of electron density able to interact unfavorably with the lone pairs of the oxygen atoms contained in to the backbone carbonyl groups. Furthermore, it is worth noting that $E^{Ph/Ph}$ is about 5 kcal/mol more repulsive in aqueous solution than in the gas phase (Table 5), indicating that the interaction of the side phenyl groups with the bulk solvent is also unfavored.

On the other hand, cyclopropane analogues of Phe bearing two phenyl groups can be directly compared with Dϕg. Recently, conformationally restricted amino acids constituted by stereoisomers of 1-amino-2,3-diphenylcyclopropanecarboxylic acid with phenyl substituents in a trans relative disposition ($c_3$diPhe; Figure 1) showed a tendency to promote folded structures in both the solid state and solution.[15,43] A systematic quantum mechanical study on Ac-(2*S*,3*S*)$c_3$diPhe-NHMe revealed that the C_7, with hydrogen-bonding parameters d(H····O) = 1.967 Å and $\angle N-H\cdots O$ = 150.6°, is the only minimum energy conformation accessible at 298 K.[15] Furthermore, an attractive interaction between the $c_3$diPhe N−H and the π cloud of the *cis*-phenyl group ($d_{H\cdots Ph}$ = 3.485 Å and θ = 4.1°) was detected for this conformation. All of the other minima were destabilized with respect to this conformation by more

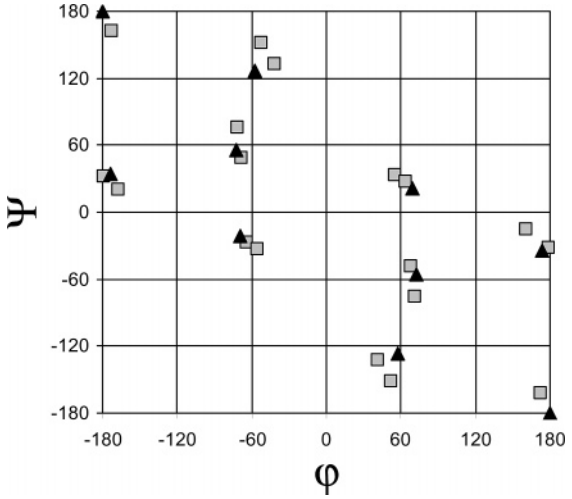

FIGURE 4. Comparison between the conformational preferences predicted for Ac-Dϕg-NHMe (squares) and Ac-Aib-NHMe (triangles) at the B3LYP/6-31+G(d,p) level.

(42) Viviani, W.; Rivail, J.-L. Perczel, A.; Csizmadia, I. G. *J. Am. Chem. Soc.* **1993**, *115*, 8321.
(43) Jiménez, A. I.; Cativiela, C.; Marroud, M. *Tetrahedron Lett.* **2000**, *41*, 5353.

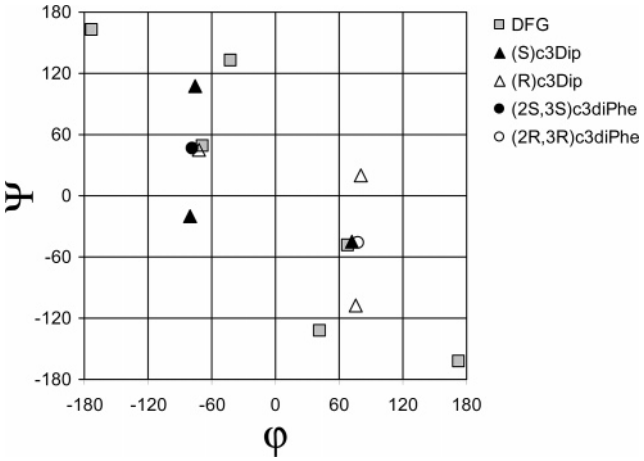

FIGURE 5. Comparison between the conformational preferences predicted for Ac-Dϕg-NHMe (squares; this work), Ac-c$_3$diPhe-NHMe (triangles; ref 15), and Ac-c$_3$Dip-NHMe (circles; ref 16). As c$_3$diPhe and c$_3$Dip are chiral amino acids, the minima associated to the two enantiomers have been differentiated.

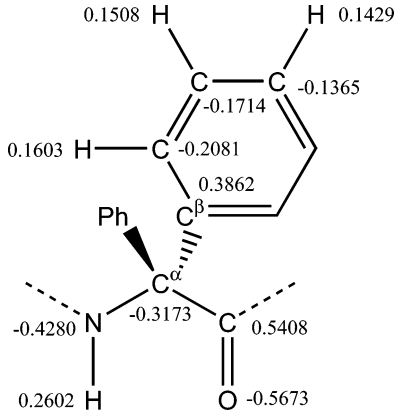

FIGURE 6. Electrostatic parameters determined for the Dϕg residue.

than 3 kcal/mol independently of the environment, i.e., gas phase, organic solution (CCl_4 and $CHCl_3$), and aqueous solution.

Very recently, quantum mechanical methods have been also used to investigate the intrinsic conformational preferences of 1-amino-2,2-diphenylcyclopropanecarboxylic acid (c$_3$Dip), a cyclopropane analogue of phenylalanine bearing two phenyl substituents on the same β-carbon.[16] Interestingly, Ac-(*S*)c$_3$Dip-NHMe showed three minima with relative energies below a threshold of 3 kcal/mol in both the gas-phase and organic solution. These correspond to the C_7 with d(H$\cdots$O) = 1.987 Å and $\angle$N−H$\cdots$O = 148.4°, the P_{II} and the α conformations, the latter two structures being destabilized with respect to the former one by 1.9 and 2.4 kcal/mol, respectively, at the B3LYP/6-31+G(d,p) level. The α minimum presents a favorable interaction between the N−H moiety of c$_3$Dip and the π-system of the *cis*-phenyl ring, no stabilizing interaction being formed by the aromatic substituents of the C_7 and P_{II} conformations.

Figure 5 compares the position in the φ,ψ-Ramachandran map of all the minima with a relative energy lower than 3 kcal/mol characterized for Ac-Dϕg-NHMe, Ac-(2*S*,3*S*)c$_3$diPhe-NHMe, and Ac-(*S*)c$_3$Dip-NHMe, the minima associated with the enantiomers of the two latter dipeptides being also represented. It is worth noting that the most remarkable difference between Dϕg and the two cyclopropane analogues of Phe corresponds to the C_5 conformation, which was only detected for the former amino acid. Indeed, this conformation is strongly unfavored for both c$_3$diPhe and c$_3$Dip because of the repulsive interaction between the π electron density of the phenyl side chains and the lone pairs of the carbonyl groups. On the other hand, the remaining minima suggest a degree of similarity among the three residues, especially around the C_7 conformation, indicating that the interactions between the backbone and the phenyl side groups are able to modulate the conformational preferences of the dipeptides. Thus, the incorporation of selectively oriented phenyl groups produces steric and electronic interactions between these rigidly aromatic groups and the peptide backbone.

Force-Field Parametrization. The stretching, bending, torsional, and van der Waals parameters used in the Amber force field to describe the phenylalanine residue were directly transferred to Dϕg,[44] the only exception being the bending parameters associated with the N−C$^\alpha$−C$^\beta$ and C$^\beta$−C$^\alpha$−C(=O) bond angles (Figure 6). The equilibrium values used to describe these angles were 110.9° and 108.5°, respectively, while the bending force constant was 63.6 kcal/mol·rad^2 in the two cases.

Atomic charges for the minimum energy conformations listed in Table 1 were calculated by fitting the HF/6-31G(d) quantum mechanical and the Coulombic molecular electrostatic potentials (MEPs) to a large set of points placed outside the nuclear region. It should be noted that the electrostatic parameters derived at this level of theory are fully compatible with the current Amber force field.[44] Electrostatic potential (ESP) fitting atomic centered charges for the Dϕg residue were derived by weighting the charges calculated for the nine minimum energy conformations, using normalized Boltzmann populations as weight factors for each minimum.[45,46] The weights were calculated by the standard Boltzmann formula using the ΔG^{gp} values listed in Table 2. This strategy based on weighted multiple conformation was previously used to determine the electrostatic parameters of several α,α-dialkylated amino acids,[13,14,47] successful results being obtained in all cases. However, it is worth noting that in this study the main contribution to the electrostatic parameters of Dϕg, which are displayed in Figure 6, arises from the C_5-I minimum, the contributions of all the other minima being negligible.

In order to ascertain how the force-field parameters describe the conformational flexibility of Ac-Dϕg-NHMe in aqueous solution, MD simulations were performed at 298 K. The lowest energy conformation was used as starting point of a trajectory that was 25 ns long. Figure 7 represents the accumulated Ramachandran plot for the Dϕg dipeptide. The most populated conformation corresponds to the C_5, which is visited approximately five times more than all the other conformations during the trajectory. This fact is in excellent agreement with the results displayed in Table 2, which indicate that this conformation is the lowest energy minimum. Moreover, all the

(44) Cornell, W. D.; Cieplak, P.; Bayly, C. I.; Gould, I. R.; Merz, K. M.; Ferguson, D. M.; Spellmeyer, D. C.; Fox, T.; Caldwell, J. W.; Kollman, P. A. *J. Am. Chem. Soc.* **1995**, *117*, 5179.
(45) Reynolds, C. A.; Essex, J. W.; Richards, W. G. *J. Am. Chem. Soc.* **1992**, *114*, 9075.
(46) Cieplak, P.; Cornell, W. D.; Bayly, C. I.; Kollman, P. A. *J. Comput. Chem.* **1995**, *16*, 1357.
(47) Alemán, C.; Casanovas, J. *J. Chem. Soc., Perkin Trans. 2* **1994**, 563.

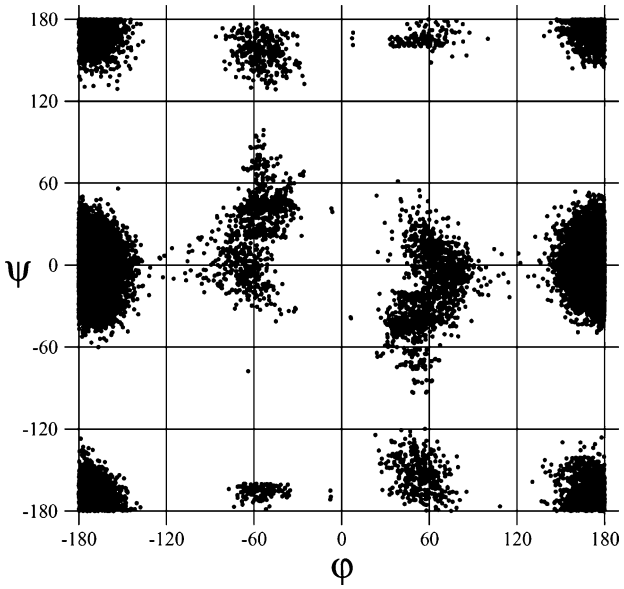

FIGURE 7. Accumulated Ramachandran plot for Ac-Dϕg-NHMe derived from a MD trajectory 25 ns long in aqueous solution.

other minimal energy conformations that had previously been predicted by DFT calculations are seldom visited during this simulation. P_{II} is the region that was less visited during the simulation, followed by the C_7 conformation and the α conformation. Considering the large number of minima characterized for Ac-Dϕg-NHMe, which reflect the complex conformational equilibrium of the Dϕg residue, we feel that the map displayed in Figure 7 is a good result.

Conclusions

DFT calculations have allowed detect a large number of minimum energy conformations for Ac-Dϕg-NHMe, many of them involving specific backbone···backbone (intramolecular hydrogen bonds) and backbone···side chain (N−H···π and C−H···π) interactions. In spite of this, the only conformations that are expected to present significant populations at room temperature in both gas-phase and aqueous solution are the C_5-I and C_7-III, the ΔG^{gp} and ΔG^{WAT} with the remaining minima being higher than 1.5 kcal/mol. Furthermore, it has been found that the phenyl substituents induce strain effects in the internal geometry of the peptide. Thus, a significant destabilizing energy contribution was obtained when the phenyl groups of Ac-Dϕg-NHMe replace the methyl groups of Ac-Aib-NHMe. On the other hand, comparison of the intrinsic conformational preferences predicted for Dϕg with those found for $c_3$diPhe and c_3-Dip reveals a degree of similarity indicating that the interactions between the phenyl and the backbone play a crucial role in the conformational preferences of the peptide. Finally, classical MD simulations in aqueous solution indicate that the set of force-field used in this work to describe the Dϕg residue are able to reproduce satisfactorily the conformational preferences of Ac-Dϕg-NHMe. These parameters were obtained by combining explicitly developed ESP charges with stretching, bending, torsional, and van der Waals parameters directly transferred from the Amber force field.

Acknowledgment. We are indebted to the Centre de Supercomputació de Catalunya (CESCA) and the Universitat de Lleida for computational resources. We acknowledge the National Cancer Institute for partial allocation of computing time and staff support at the Advanced Biomedical Computing Center of the Frederick Cancer Research and Development Center. Classic calculations were partially formed by utilizing the high-performance computational capabilities of the Biowulf PC/Linux cluster at the National Institutes of Health, Bethesda, MD (http://biowulf.nih.gov). D.Z. acknowledges financial support from the "Ramon y Cajal" program of the Spanish "Ministerio de Educación y Ciencia" (MEC). This project has been funded in whole or in part with federal funds from the National Cancer Institute, National Institutes of Health, under contract no. N01-CO-12400. The content of this publication does not necessarily reflect the view of the policies of the Department of Health and Human Services, nor does mention of trade names, commercial products, or organization imply endorsement by the U.S. Government. This research was supported (in part) by the Intramural Research Program of the NIH, National Cancer Institute, Center for Cancer Research.

Supporting Information Available: Coordinates, energy, and free energy of the minimum energy conformations characterized for Ac-Dϕg-NHMe. This material is available free of charge via the Internet at http://pubs.acs.org.

JO0624905